Sixth Portuguese Conference on Automatic Control

Faro, Portugal, June 7-9

Organized by

FRACTIONAL-ORDER POSITION AND FORCE ROBOT CONTROL

N. M. Fonseca Ferreira, J. A. Tenreiro Machado, J. Boaventura Cunha

Dept. of Electrical Engineering Institute of Coimbra, Rua Pedro Nunes - Quinta da Nora 3031-601 Coimbra Codex, Portugal, email: nunomig@isec.pt
Dept. of Electrical Engineering, Institute of Engineering of Porto, Rua Dr Ant. Bernardino de Almeida 4200-072 Porto Codex, Portugal, email: jtm@dee.isep.ipp.pt
Dept. of Electrical Engineering, University of Trás dos Montes e Alto Douro, Ap 1013, 5000-911 Vila Real, Portugal, email: jboavent@utad.pt

Abstract: This paper presents the implementation of fractional-order algorithms both for hybrid and cascade position/force control of robotic manipulators. The system performance and robustness is analyzed in the time domain. The impact effects of the robot gripper with the environment are also investigated.

Keywords: Robot, position/force control, impacts.

1. Introduction

In this early eighties (Raibert and Craig 1981) introduced the concept of force control based on the hybrid algorithm. Since then, several researchers (O. Khatib 1987) developed these ideas and proposed new algorithms such as the impedance controller. Problems with position/force control are further investigated in required (Hogan, 1985) while more recent studies of this algorithm can be found in (Siciliano, 1999).
There are two basic methods for force control, namely the hybrid position/force and the impedance schemes. The first algorithm (Raibert and Craig 1981) separates the task into two orthogonal subspaces corresponding to the force and the position subspaces. Once established the subspace decomposition two independent controllers are designed. Alternatively, with the second algorithm (Hogan, 1985), by a proper choice of the arm impedance, the interaction forces can be accommodated to obtain an adequate response.
This paper studies the position/force control of robot manipulators, required in processes that involve contact between the gripper and the environment, using fractional-order (*FO*) algorithms. The application of the theory of fractional calculus is still in a research stage, but the recent progress in this area reveals promising aspects for future developments (Oustaloup, 1995, Pondlubny, 1999, Ferreira and Machado, 2003).

In this line of thought the article is organized as follows. Sections two and three introduce the hybrid controller (*HC*) and the position/force cascade controller (*CC*) and the fundamentals of the *FO* algorithms, respectively. Section four analyses several experiments for the performance evaluation of two strategies, considering the robot impacts, for different working surfaces. Finally, section five outlines the main conclusions.

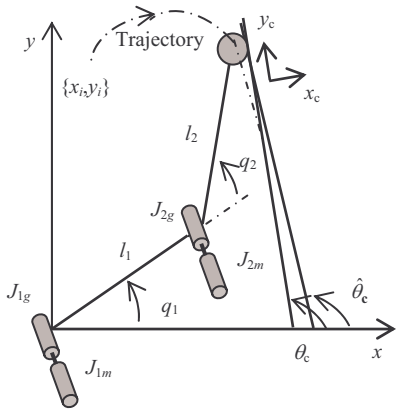

Figure 1 – The 2*R* robot and the constraint surface.

2. The Hybrid and Cascade Controllers

The dynamical equations of a n dof robot are:

$$\boldsymbol{\tau} = \mathbf{H}(\mathbf{q})\ddot{\mathbf{q}} + \mathbf{C}(\mathbf{q},\dot{\mathbf{q}}) + \mathbf{G}(\mathbf{q}) - \mathbf{J}^{\mathbf{T}}(\mathbf{q})\mathbf{F} \tag{1}$$

where $\boldsymbol{\tau}$ is the $n \times 1$ vector of actuator torques, $\mathbf{q}$ is the $n \times 1$ vector of joint coordinates, $\mathbf{H(q)}$ is the $n \times n$ inertia matrix, $\mathbf{C(q,\dot{q})}$ is the $n \times 1$ vector of centrifugal/Coriolis terms and $\mathbf{G(q)}$ is the $n \times 1$ vector of gravitational effects. The $n \times m$ matrix $\mathbf{J^T(q)}$ is the transpose of the Jacobian of the robot and $\mathbf{F}$ is the $m \times 1$ vector of the force that the (m-dimensional) environment exerts in the gripper.

In this study we adopt the 2R robot (Fig. 1) with dynamics given by (n = 2):

$$\mathbf{H}(\mathbf{q}) = \begin{bmatrix} m_1 + m_2\, r_1^{\,2} + m_2 r_2^{\,2} + 2m_2 r_1 r_2 C_2 + J_{1m} + J_{1g} & m_2 r_2^{\,2} + m_2 r_1 r_2 C_2 \\ m_2 r_2^{\,2} + m_2 r_1 r_2 C_2 & m_2 r_2^{\,2} + J_{2m} + J_{2g} \end{bmatrix} \tag{2a}$$

$$\mathbf{C}(\mathbf{q},\dot{\mathbf{q}}) = \begin{bmatrix} -m_2 r_1 r_2 S_2 \dot{q}_2^{\,2} - 2m_2 r_1 r_2 S_2 \dot{q}_1 \dot{q}_2 \\ m_2 r_1 r_2 S_2 \dot{q}_1^{\,2} \end{bmatrix} \tag{2b}$$

$$\mathbf{G}(\mathbf{q}) = \begin{bmatrix} g m_1 r_1 C_1 + m_2 r_1 C_1 + m_2 r_2 C_{12} \\ g m_2 r_2 C_{12} \end{bmatrix} \tag{2c}$$

$$\mathbf{J^T}(\mathbf{q}) = \begin{bmatrix} -r_1 S_1 - r_2 S_{12} & r_1 C_{11} + r_2 C_{12} \\ -r_2 S_{12} & r_2 C_{12} \end{bmatrix} \tag{2d}$$

where $C_{ij} = \cos(q_i + q_j)$ and $S_{ij} = \sin(q_i + q_j)$.

The numerical values adopted for the robot are m_1 = 0.5 kg, m_2 = 6.25 kg, r_1 = 1.0 m, r_2 = 0.8 m, $J_{1m} = J_{2m}$ = 1.0 kgm^2 and $J_{1g} = J_{2g}$ = 4.0 kgm^2.

The constraint plane is determined by the angle θ_c (Fig. 1) and the contact displacement x_c of the robot gripper with the constraint surface is modeled through a linear system with a mass M, a damping B and a stiffness K with dynamics:

$$F_c = M\ddot{x}_c + B\dot{x}_c + Kx_c \tag{3}$$

The first control architecture consists on the *HC* algorithm (Fig. 2). The diagonal $n \times n$ selection matrix $\mathbf{S}$ has elements equal to one (zero) in the position (force) controlled directions and $\mathbf{I}$ is the $n \times n$ identity matrix. In this paper the y_c (x_c) cartesian coordinate is position (force) controlled, yielding:

$$\mathbf{S} = \begin{bmatrix} 0 & 0 \\ 0 & 1 \end{bmatrix},\ \mathbf{J_c}(\mathbf{q}) = \begin{bmatrix} -r_1 C_{\theta 11} - r_2 C_{\theta 12} & -r_2 C_{\theta 12} \\ r_1 S_{\theta 11} + r_2 S_{\theta 12} & r_2 S_{\theta 12} \end{bmatrix} \tag{4}$$

where $C_{\theta ij} = \cos(\theta_c - q_i - q_j)$ and $S_{\theta ij} = \sin(\theta_c - q_i - q_j)$.

The *CC* architecture (Fig. 3) is inspired on the impedance and compliance schemes. Therefore, we establish a cascade of force and position algorithms as internal an external feedback loops, respectively, where $\boldsymbol{x}_\mathbf{d}$ and $\boldsymbol{F}_\mathbf{d}$ are the payload desired position coordinates and contact forces.

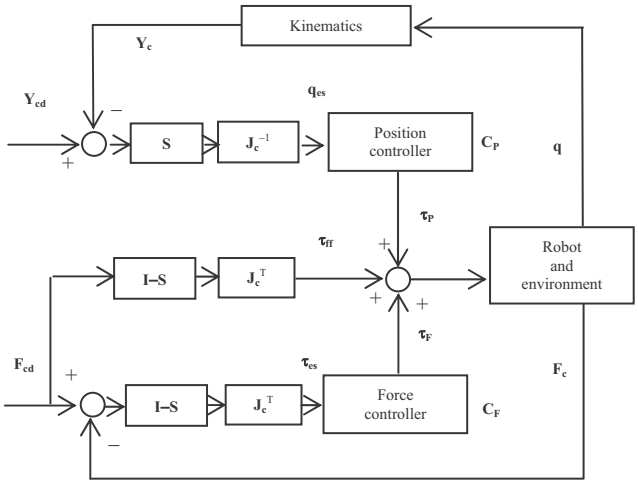

Figure 2 – The position/force hybrid controller.

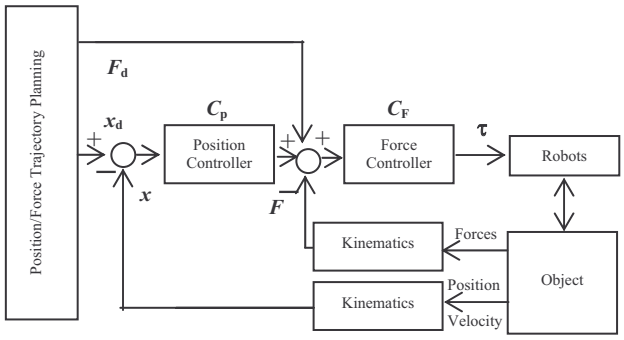

Figure 3 – The position/force cascade controller.

3. Fractional Order Algorithms

In this section we present the *FO* algorithms inserted in the position and force control loops.
The mathematical definition of a derivative of fractional order α has been the subject of several different approaches. For example, we can mention the Laplace and the Grünwald-Letnikov definitions:

$$D^{\alpha}[x(t)] = L^{-1}\{s^{\alpha} X(s)\} \tag{5a}$$

$$D^{\alpha}[x(t)] = \lim_{h \to 0}\left[\frac{1}{h^{\alpha}} \sum_{k=1}^{\infty} \frac{(-1)^k\, \Gamma(\alpha + 1)}{\Gamma(k+1)\,\Gamma(\alpha - k + 1)}\, x(t - kh)\right] \tag{5b}$$

where Γ is the gamma function and h is the time increment.

In our case, for implementing *FO* algorithms of the type $C(s) = K\,(s+\lambda)^{\alpha}$, $-1 < \alpha < 1$, we adopt a $k = 4$ discrete-time Pade approximation (a_{Pi}, b_{Pi}, a_{Fi}, $b_{Fi} \in \Re$):

$$C_P(z) \approx K_P \sum_{i=0}^{k} a_{Pi} z^i \Big/ \sum_{i=0}^{k} b_{Pi} z^i \qquad (6a)$$

$$C_F(z) \approx K_F \sum_{i=0}^{k} a_{Fi} z^i \Big/ \sum_{i=0}^{k} b_{Fi} z^i \qquad (6b)$$

where K_P and K_F are the position and force loop gains.

4. Controller Performances

This section analyzes the system performance for the two controller architectures. Both algorithms were tuned by trial and error having in mind getting a similar performance in the two cases. By other words, the gains were adjusted not only to get small overshoots and steady state errors, but also to have similar responses of the *HC* and *CC* in order to easy the performance comparison. The resulting parameters were for the *HC–FO*: $\{K_P, \lambda_P, \alpha_P\} \equiv \{110, 120, 0.5\}$, $\{K_F, \lambda_F, \alpha_F\} \equiv \{142, 130, -0.2\}$ and for the *CC–FO*: $\{K_P, \lambda_P, \alpha_P\} \equiv \{5.9, 100, 0.5\}$, $\{K_F, \lambda_F, \alpha_F\} \equiv \{30, 177, -0.2\}$ for the position and force loops, respectively.

It is adopted a loop trajectory starting at the operating point $\{x_i,y_i\} \equiv \{1,1\}$, in the open space, and approximately after one second there is a contact with the constraint surface. The other parameters are $\{\theta_c,M,B,K\} \equiv \{45^o,10^3,1.0,10^2\}$, a contact reference force with the surface restriction of $Fx_c \equiv 10$ *Nm* and a controller sampling frequency $f_c = 1$ kHz.

In order to study the system dynamics we apply, separately, rectangular pulses, at the position and force references, that is, we perturb the references with $\{\delta y_{cd}, \delta F_{cd}\} = \{10^{-3}, 0\}$ and $\{\delta y_{cd}, \delta F_{cd}\} = \{0, 10^{-2}\}$. In both cases the estimated angle of the surface restriction $\hat{\theta}_c$ is varied to study the control system performance.

Figures 4 to 9 depict the robot time response under the action of the *FO* algorithm, both for the *HC* and *CC* architectures, when $\hat{\theta}_c = \theta_c$ and $\hat{\theta}_c \neq \theta_c$. In particular, Figures 6 and 9 analyze the influence of an inaccurate estimate of θ_c upon the square trajectory errors ε defined as:

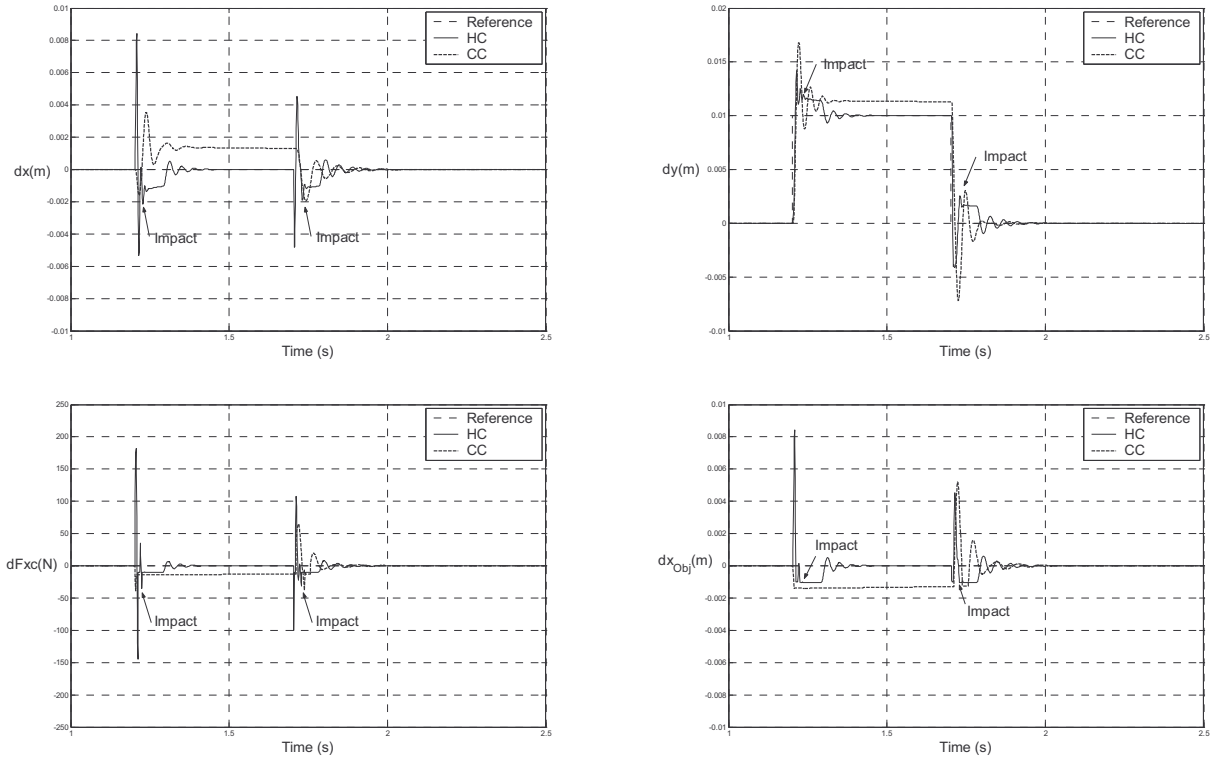

Figure 4 – Time response for the 2*R* robot under the action of the *FO* algorithm for the *HC* and the *CC*, $\delta y_d = 10^{-3}$m, $\hat{\theta}_c = \theta_c = 45$ degree.

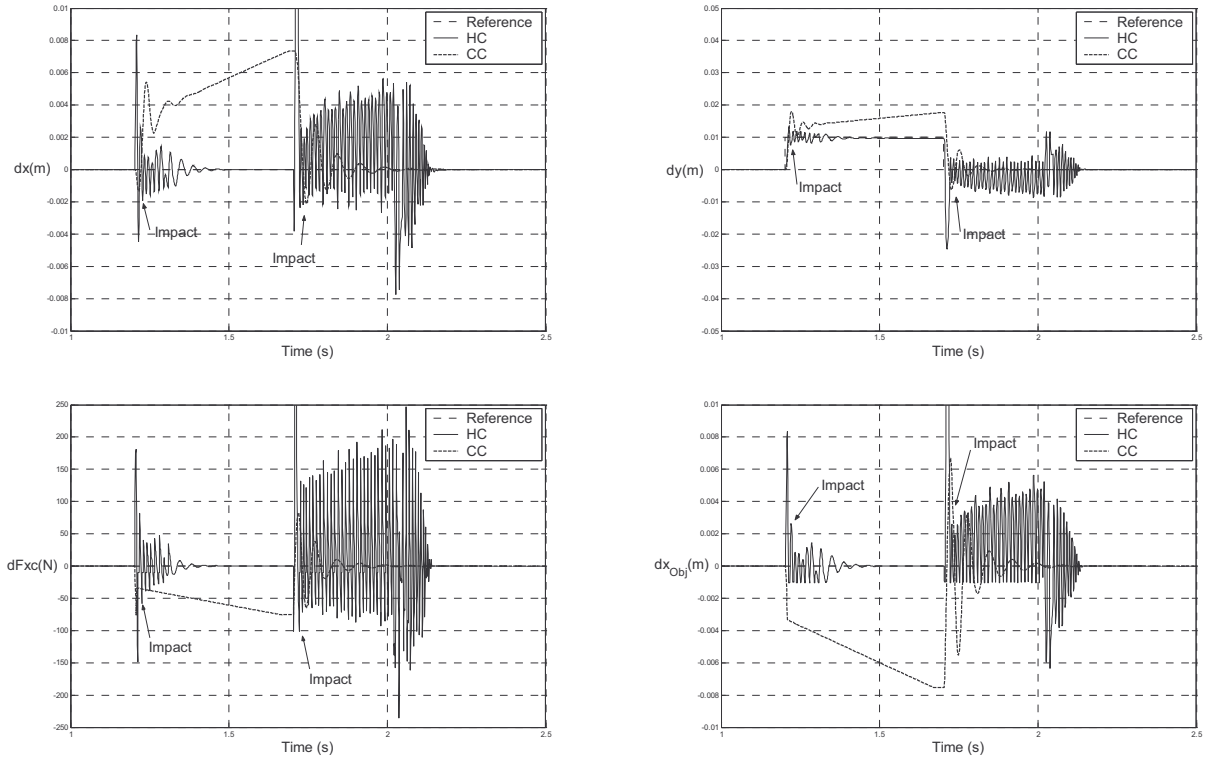

Figure 5 – Time response for the 2*R* robot under the action of the *FO* algorithm for the *HC* and the *CC*, $\delta y_d = 10^{-3}$m, $\hat{\theta}_c = 46$ degree.

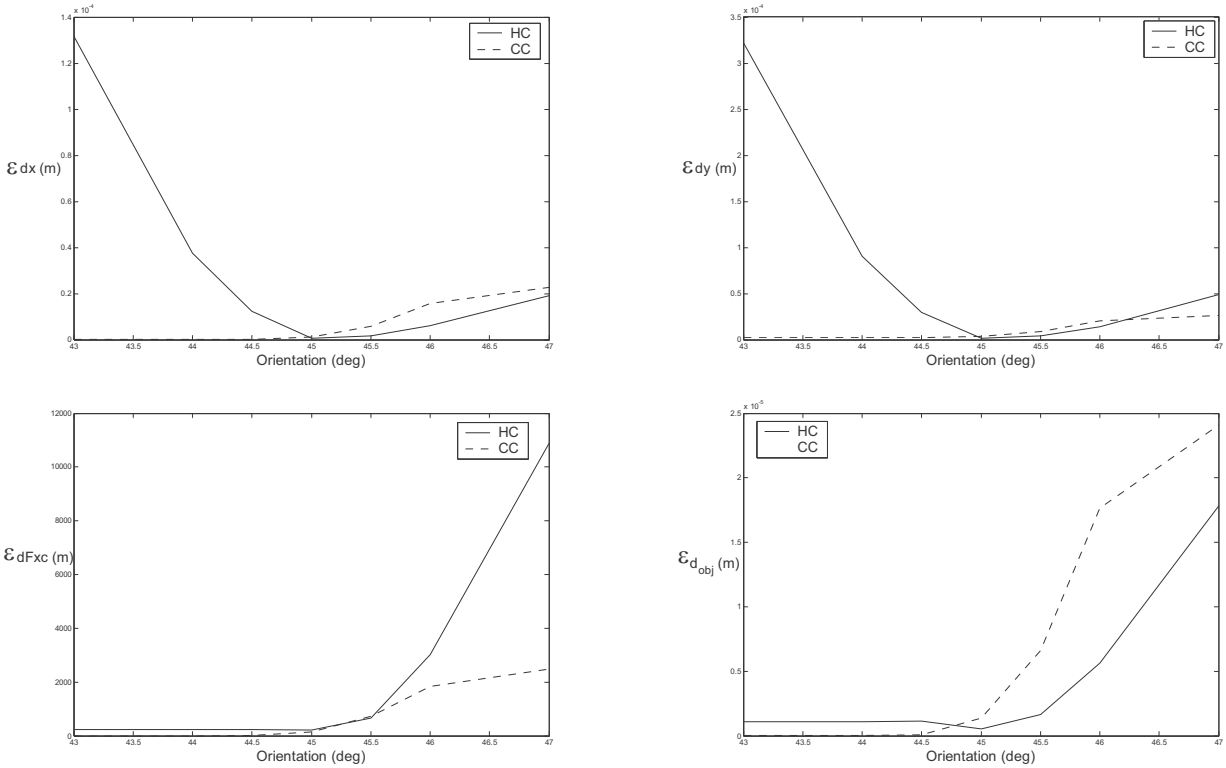

Figure 6 – The square error of the time response ε *versus* the estimation orientation angle $\hat{\theta}_c$ for the *HC* and the *CC* with $\delta y_d = 10^{-3}$ m.

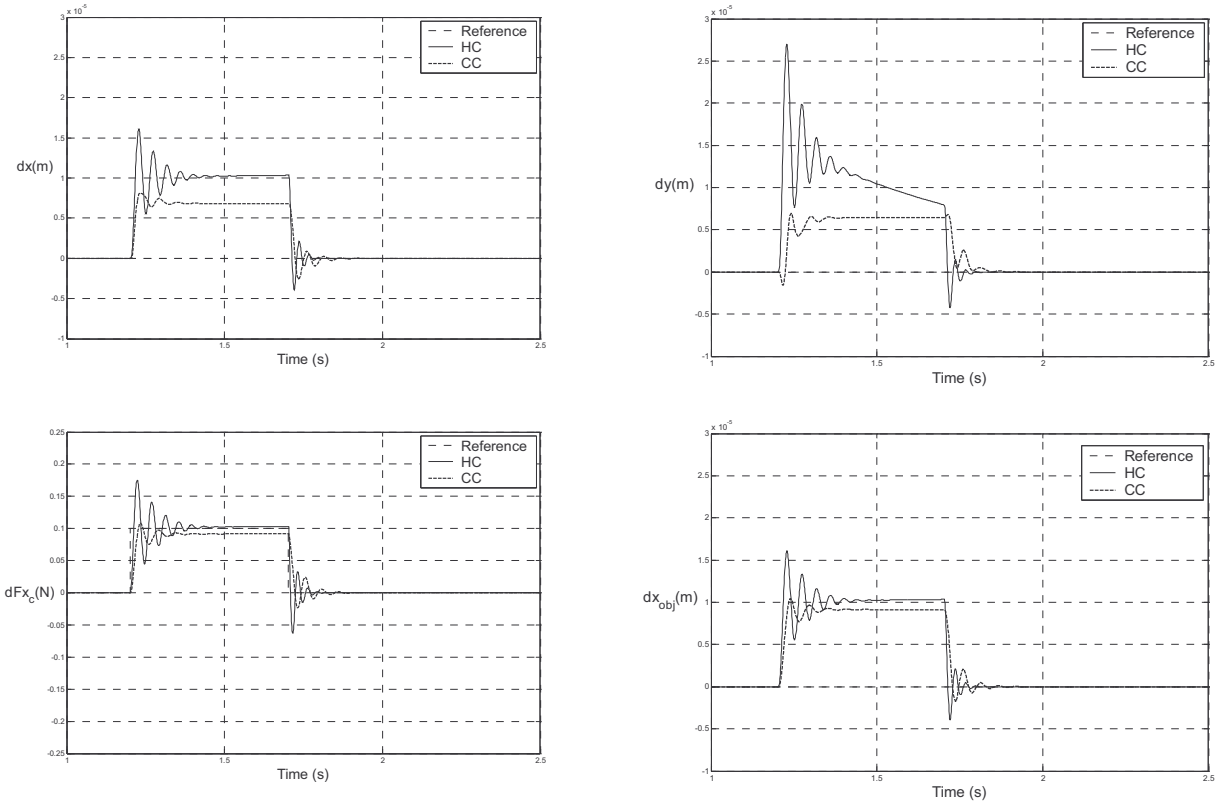

Figure 7 – Time response for the 2*R* robot under the action of the *FO* algorithm for the *HC* and the *CC*, $\delta F_d = 10^{-2}$N, $\hat{\theta}_c = \theta_c = 45$ degree.

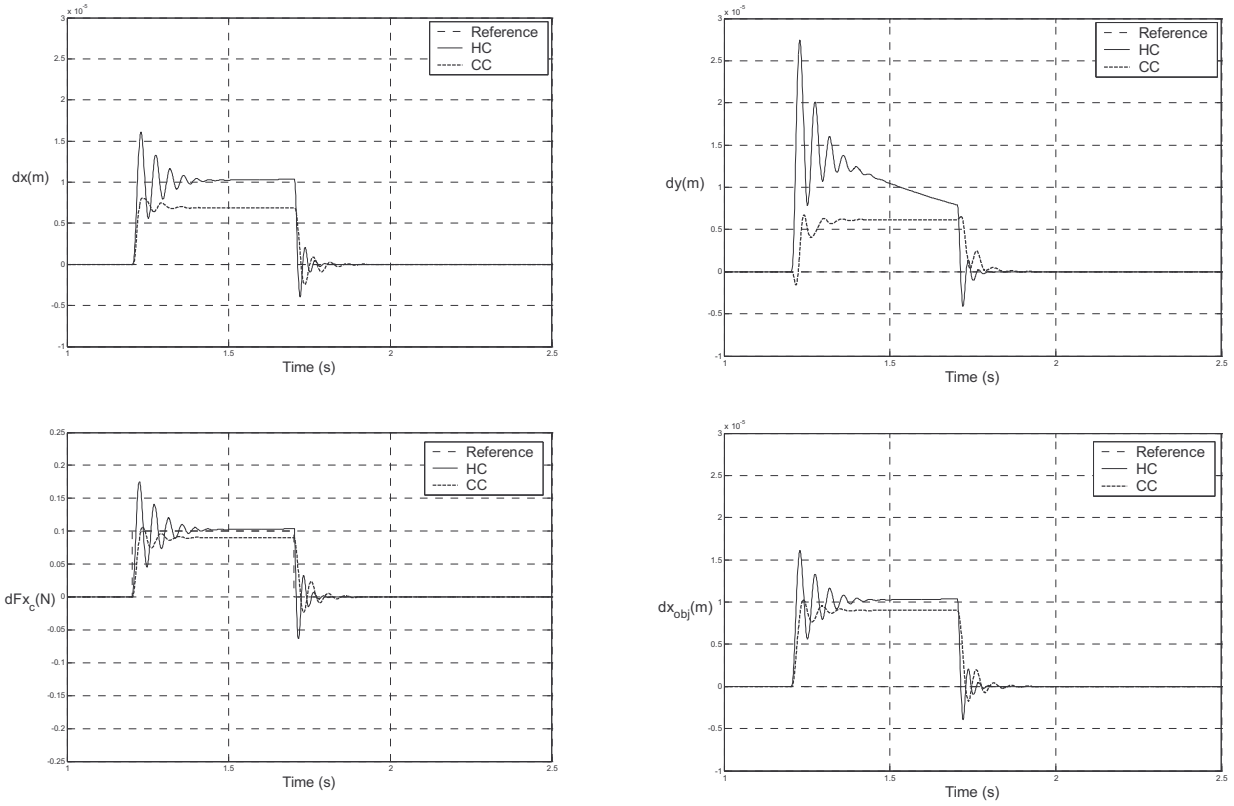

Figure 8 – Time response for the 2*R* robot under the action of the *FO* algorithm for the *HC* and the *CC*, $\delta F_d = 10^{-2}$N, $\hat{\theta}_c = 46$ degree.

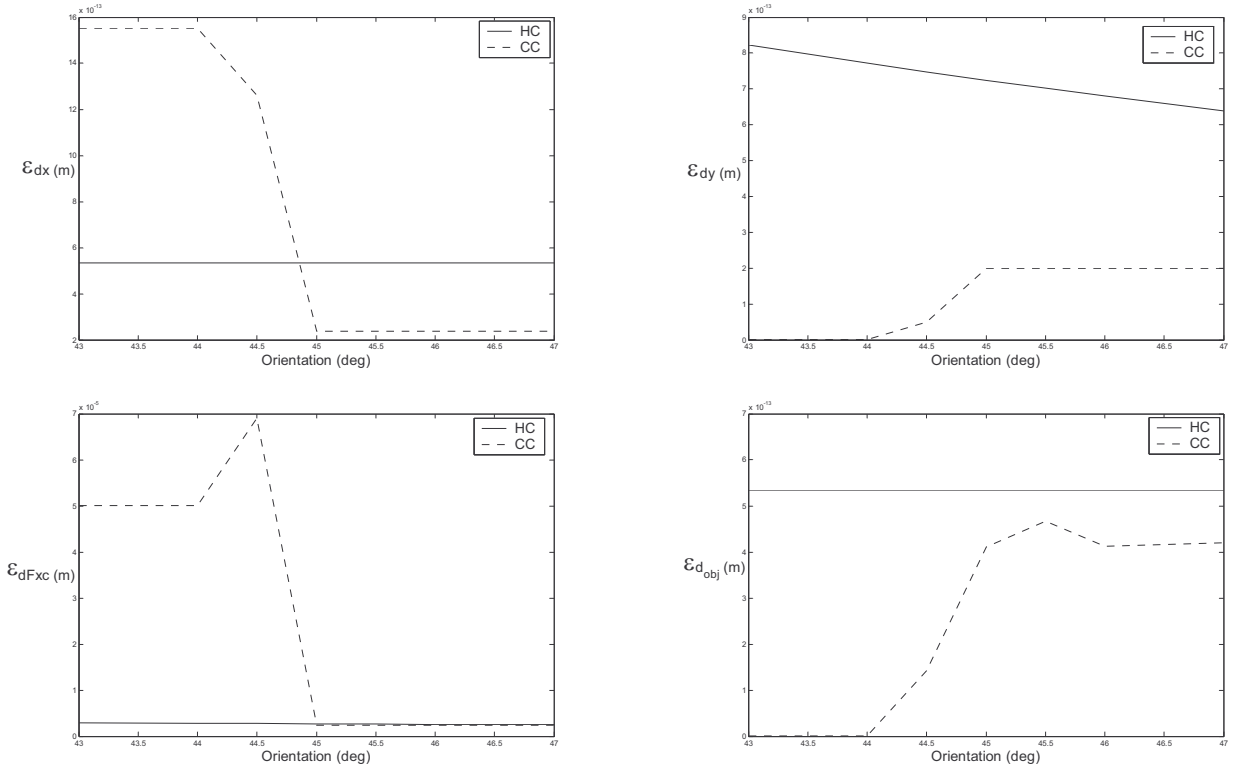

Figure 9 – The square error of the time response ε *versus* the estimation orientation angle $\hat{\theta}_c$ for the *HC* and the *CC* with $\delta F_d = 10^{-2}$ N.

$$\varepsilon = \int_0^{+\infty} [\delta(t) - \delta^*(t)]^2 dt \qquad (7)$$

where $\varepsilon \equiv \{\varepsilon\delta x,\ \varepsilon\delta y,\ \varepsilon\delta Fx_c,\ \varepsilon\delta x_{obj}\}$ and δ and δ^* represent the corresponding perturbations in the variables $\{\delta x,\ \delta y,\ \delta Fx_c,\ \delta x_{obj}\}$ when $\hat{\theta}_c = \theta_c$ and $\hat{\theta}_c \neq \theta_c$, respectively.

In Figures 5 and 8 it is clear the effect of the impact of the robot with the surface restriction for the *HC*. The main cause of this large collision is the difference between the estimated $\hat{\theta}_c$ and the real value θ_c of contact surface. We conclude also that the *HC* has a smaller steady-state error in the position reference, but has higher transient oscillations. On the other hand, the *CC* has a superior stability and good adaptation with the surface variations.

5. Summary and Conclusions

This paper presented the implementation of the hybrid and the cascade algorithms, in force/position control, in order to study the impact of the robot with the surface. The cascade control reveals better adaptation in robot position/force control and superior robustness to an inaccurate estimate of the working surface location.

References

M. H. Raibert and J. J. Craig, (1981), "Hybrid Position/Force Control of Manipulators", *ASME J. of Dynamic Systems, Measurement, and Control*" vol. 2, No. 2, pp.126-133, vol. 1.

N. Hogan, (1985) "Impedance control: An Approach to Manipulation, Parts I-Theory, II-Implementation, III-Applications", *ASME J. of Dynamic Systems, Measurement and Control*, vol. 107, No. 1, pp. 1-24.

B. Siciliano and L. Villani, (1999) "Robot Force Control", *Kluwer Academic Publishers*.

O. Khatib, (1987) "A Unified Approach for Motion and Force Control of Robot Manipulators: The Operational Space Formulation", *IEEE Journal of Robotics and Automation*, vol. 3, no. 1, pp. 43–53.

N. M. Fonseca Ferreira and J. A. Tenreiro Machado, (2003), "Fractional-Order Hybrid Control of Robotic Manipulator", *Proceedings of the 11th IEEE Int. Conf. on Advanced Robotics, Coimbra, Portugal*.

A. Oustaloup, (1995) *La Dérivation Non Entière: Théorie, Synthèse et Applications*, Hermes, Paris.

J. Tenreiro Machado, (1997) "Analysis and Design of Fractional-Order Digital Control Systems", *J. Systems Analysis, Modelling and Simulation*, vol. 27, pp. 107–122.

I. Podlubny, (1999) "Fractional-Order Systems and $PI^{\lambda}D^{\mu}$-Controllers", *IEEE Trans. on Automatic Control*, vol. 44, no. 1, pp. 208–213.

S. Dubowsky, J. F. Deck and H. Costello, (1987) "The Dynamic Modelling of Flexible Spatial Machine Systems with Clearance Connections", *ASME Journal of Mechanisms, Transmissions and Automation in Design,* vol. 109, no. 1, pp. 87–94.